CHEMICAL ENGINEERING TRANSACTIONS
VOL. 48, 2016

A publication of AIDIC
The Italian Association of Chemical Engineering
Online at www.aidic.it/cet

Guest Editors: Eddy de Rademaeker, Peter Schmelzer

ISBN 978-88-95608-39-6; ISSN 2283-9216
DOI: 10.3303/CET1648093

# CO2 Transportation Hazards in CCS and EOR Operations: Preliminary Lab – scale Experimental Investigation of CO2 Pressurized Releases

Paolo Mocellin, Chiara Vianello, Giuseppe Maschio*

University of Padova, Department of Industrial Engineering, via Marzolo 9, 35131 Padova, Italy
giuseppe.maschio@unipd.it

An experimental apparatus has been built in order to perform $CO_2$ releases under controlled conditions. It is made of a dedicated 2,25 l tank made of stainless steel in which the $CO_2$ can be introduced at pressures up to 110 bar. A discharge line consisting of a 0.125 in internal diameter pipe carries the $CO_2$ out of the pressurized tank to an atmospheric environment. The discharge line, as well as the tank interior, is monitored by an arrangement of specific high – frequency pressure sensors and thermocouples in order to collect pressure and temperature profiles during the rapid depressurization.
The aim of this study is to collect further experimental data concerning the rapid discharge of gaseous $CO_2$ from a high pressure reservoir. This should help to better understand the compressible transient fluid behaviour in the vessel and along the discharge line. This to support hazard investigation and modelling activities applied to accidental releases of $CO_2$ during transportation operations. The implementation of a theoretical discharge model as well as the analysis of the main feature of the jet is delegate to future works.
In this preliminary analysis and tuning stage, pressure and temperature profiles during the rapid depressurization from varying initial pressures are collected together with the external surface temperatures in order to investigate the main features of the expansion. This in order to preliminary assess how the system designed behaves during the depressurization.

## 1. Introduction

Infrastructures carrying gaseous and dense $CO_2$ are of recent introduction and represent peculiar elements of the development of the CCS (Carbon Capture and Storage) and EOR (Enhanced Oil Recovery) techniques (Martynov et al., 2014). The transportation step is characterized by the handling of huge amounts of $CO_2$ that are moved from the capture to the storage location through a dedicated network of pipelines.
However the deficiency in the number of installed infrastructures and therefore in their management experience makes it difficult to schedule a proper and comprehensive hazards analysis (Mocellin et al., 2015). Main difficulties arise when dealing with the modeling and the prediction of the pressurized discharge of $CO_2$ that is a preliminary and essential QRA step linked to the consequences estimation. In fact the quantitative definition of the release scenarios involving the $CO_2$ in terms, for example, of discharge rates and total quantity released (or total release duration) is usually affected by many uncertainties.
As discussed in some works (Martynov et al., 2014; Ahmad et al., 2013a) there is a huge lack regarding the amount of reliable experimental information on transient $CO_2$ releases. This deficiency is reflected on the difficulty in setting up reliable models able to describe the complicated behavior of the discharging $CO_2$ that may lead to multi – phase releases. In addition the applicability of the HEM approach (Homogeneous Equilibrium Model) as well as the understanding of the thermodynamic depressurization path followed by the $CO_2$ is still under debate. Therefore actual release models for predicting $CO_2$ outflow from a containment need experimental data to be improved and to be able to describe correctly its rapid discharge from a pressurized reservoir (Vianello et al., 2012). In the present work a preliminary experimental investigation at lab - scale is carried out in order to study the behavior of the $CO_2$ discharged from a pressurized vessel from a thermal and

Please cite this article as: Mocellin P., Vianello C., Maschio G., 2016, Co2 transportation hazards in ccs and eor operations: preliminary lab – scale experimental investigation of co2 pressurized releases., Chemical Engineering Transactions, 48, 553-558 DOI:10.3303/CET1648093

hydraulic perspective. The tank is filled with gaseous $CO_2$ at different initial pressures which is collected from a larger reservoir maintained at controlled conditions.

## 2. Experimental set up

The data series are collected through an experimental apparatus mainly composed by a storage tank, a discharge line and a set of measurement devices as depicted in figure 1. The discharge line is equipped with two valves in order to keep the system under control during the rapid depressurization.

### 2.1 $CO_2$ reservoir

The $CO_2$ is discharged from a dedicated cylindrical vessel made of 304L austenitic stainless steel with chromium content of 18 %. Its compatibility with the gaseous $CO_2$ is excellent. It has a volume of 2.25 l and it is sized in order to bear pressures up to 110 bar. Its sizing has also taken into account the behaviour at low temperatures through thermal contraction phenomena.The tank safety is guaranteed by the presence of a calibrated spring safety valve.

### 2.2 Discharge line

The outflow of $CO_2$ is made through a 316 stainless steel line with an outside diameter of 1/8 in. The line is perfectly straight in order to minimize and to control friction losses during the discharge. As will be discussed later, main frictional losses are represented by the concentrated losses in the constriction between the tank and the line and those distributed on the whole discharge line. The discharge line is equipped with two ball valves of the same internal section of the line. The one positioned at the end of the line is devoted to the discharge in the atmospheric environment. The line is not externally thermally insulated allowing for conductive and convective heat transfer mechanisms across the material and with the surrounding air.

### 2.3 Measurement devices

Sensor devices are installed in the tank containing the $CO_2$ and along the discharge line.
The setup is dedicated to pressure and temperature measurements.

a. Pressure measures:
- vessel pressure (along the charging line)
- discharge line pressure (just downstream of the constriction and in correspondence of the discharge valve)

b. Internal temperature measures:
- vessel internal temperature
- discharge line temperature (coupled with pressure measurements)

c. Wall temperature measures:
- top of the tank
- external surface of the discharge pipe opposite the internal thermocouple.

Pressure sensors are selected in order to give high accuracy coupled with fast response time and sampling rate. Therefore pressure sensors installed in the most problematic sections (i.e. the discharge line) are characterized by a sampling rate up to 10 kHz with an accuracy of 0.05 %. They are also temperature compensated in order to be suitable to make accurate measurements in the range between – 80 and 100 °C. Temperatures are collected by using type T thermocouples with different diameters in order to govern the response time. So in places where rapid and wide temperature fluctuations are expected, thinner thermocouples are used. Type T Cu – Ni thermocouples are suitable to work in the range from -200 to 400 °C with a sensibility of 48.2 μV $°C^{-1}$. Pressure sensors and thermocouples are logged with two distinct acquisition modules. Pressure and temperature samples are collected with a frequency respectively of 40 kHz and 0.8 kHz. Measurement noise is avoided by a filtering procedure.

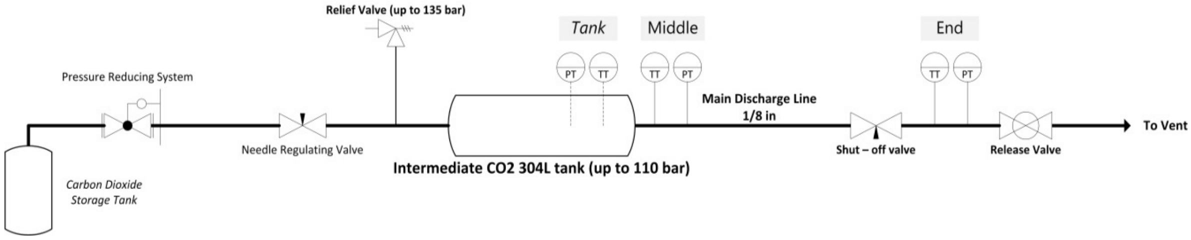


*Figure 1: schematic representation of the experimental apparatus.*

## 3. Experimental results

The experimental campaign presented in this work is primarily related to the investigation of the influence of $CO_2$ charging pressure on pressure and temperature profile in time as well as on the total discharge time. The charging pressure range is bounded between 1 and 45 barg with reference to the atmospheric value and the tank temperature is equal to 20 °C. All experimental tests took place in an indoor environment characterized by no sensible air circulation and a degree of humidity around 60 %.
Results are presented in next sections and time profiles are grouped with reference to the three locations of measurement devices as indicated in fig. 1. They are categorized respectively as *tank*, *middle* and *end* location.

### 3.1 Pressure time profiles

Transient pressure profiles are characterized by a similar shape throughout the different trials.
As an example, figure 2-a gives the pressure profiles as function of time starting from an initial storage pressure of 40 barg.

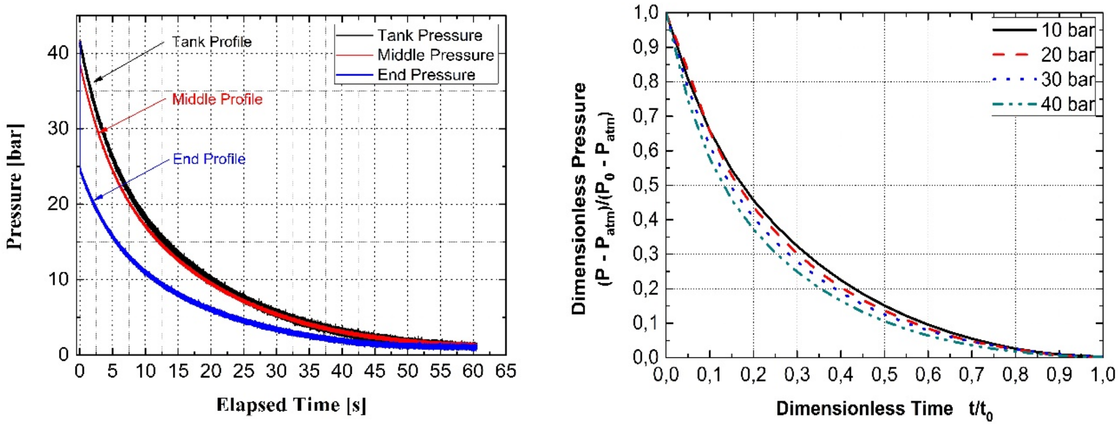


a b

*Figure 2-a: Transient pressure profiles in the tank, middle and end location. Depressurization from 40 bar. Figure 2-b: Dimensionless tank pressure profiles as function of the dimensionless time. Parameterization in the initial tank pressure.*

Following the pressure trend indicated in figure 2-a it is possible to state that the pressure trend inside the tank and just downstream of the constriction are of similar shape. The decreasing trend is very smooth and tends to reach the atmospheric pressure value at the end of the trial. Similar behaviours were detected in all the tests performed even with varying initial pressure.
Although a similar behaviour in time, it should be noted that the pressure profile collected at the end of the depressurization line is characterized by pressure values significantly lower. This is mainly due by friction losses along the depressurization path linked to the presence of concentrated and distributed loss sources (sudden shrinkage, valves and the discharge conduit). The profiles obtained from the difference represent the pressure drop trend in time between the spatial points under analysis. With reference to the experimental setup it should be noted that the pressure difference profile between the tank and the middle location pressure is mainly due to the constriction in the depressurization path. In addition, given the considerable constriction in the flow section, friction losses amount even to 3 bara and this is the location where temperature measurements record the lowest values. Results show that the amount of concentrated losses decreases lowering the initial storage pressure. The remaining losses are due to the flow inside the discharge pipe and represent the main source of pressure drop as indicated by the significant difference in the profiles.
Going back to the regular shape of the profile one can deduce the absence of boiling mechanisms in the sense that the whole release involve only gaseous phase inside the tank. In fact the profile is substantially free of persisting slope alterations that may be primarily related to phase change mechanisms when the effect of mass loss is partially compensated by the boiling liquid (Ahmad et al., 2013b). Additional observations will be made later in section 3.3 when dealing with the pressure – temperature depressurization path.
A comparison between different depressurization trials can be made resorting to dimensionless variables being the duration of test strongly influenced by the initial pressure. Profiles resulted are depicted in figure 2-b. Therefore, with the exception of the profile for $t^* < 0.06$, the profiles of the dimensionless pressure display different trends depending on the initial pressure in the tank. This means that varying the initial storage

pressure the depressurization follows different paths and once increased, at the same dimensionless time the pressure recorded is lower. While the middle profile exhibits similar trends, results concerning the *end* location are much more conditioned by the initial operative pressure. In fact an increase in the initial pressures is strictly linked to higher flow velocities and therefore larger distributed friction losses that acts directly on the pressure trends.

### 3.2 Temperature profiles

Trials have shown that the temperature trend is more complicated exhibiting a much less regular trend although substantially generalizable to the various test.

From a thermodynamic point of view one must expect a drop in temperature when dealing with the depressurization. However the nature of the expansion cannot be established a priori being this strictly linked to the heat transfer occurring during the transformation. Internal thermocouples installed on the experimental setup have collected data reported in figure 3-a (solid lines), for a depressurization starting from 40 bar.

Trends obtained display marked differences both in the temperature dynamics and in its change magnitude. The tank temperature dynamics is the slowest reaching its minimum value after 40 s while the middle location just downstream of the constriction is characterized by faster temperature dynamics. Experimental results shows that the minimum temperature value reached remains almost unchanged between these two locations meaning that the cooling expansion mechanism takes place in this section of the equipment.

On the other hand the farthest location is characterized by more limited decreases in the temperature.

This is explained considering that the flow in the discharge line is characterized by a significant heat transfer mainly driven by the high speed flow and the heat exchanged with the pipe material. In this sense the wall temperature sensors prove an exchange dynamic absolutely not negligible as indicated in figure 3-a (dashed lines). While the tank wall maintains almost the same temperature, the solid body in the middle and end location undergoes a relevant drop in temperature. Sensors are placed on the external surface and, given the high conductivity of the stainless steel, values collected can be taken as local average neglecting internal temperature gradients.

Figure 3-a shows that the drop in the gas temperature driven by the decrease in the pressure leads to a cooling of the solid mass the latter therefore representing a local heat reservoir. Therefore temperatures reached by the gas without this heat exchange would definitely be lower corresponding to an ideal adiabatic expansion. It should be observed that at the same time value, the temperature is much lower downstream of the constriction point as further confirmation of the equipment section interested by the temperature drop. This is also related to the smaller heat capacity of the local solid body compared to the tank one.

With the progress of the tests is possible to observe that the internal and wall temperature trends in the *middle* and *end* locations tend to overlap moving to the equilibrium state with the external air temperature. The same tank dynamics is much slower and this mainly due to the thermal inertia of the huge stainless steel structure.

In addition figure 3-b gives the minimum temperature reached inside the tank as function of the initial pressure. The trend is characterized by two distinct region with the first represented by an almost linear drop (up to 20 barg) and the second with an apparent decrease in slope. Further investigations are underway with the aim of completing the profile to better understand the nature of this behaviour that will be coupled with a mathematical model.

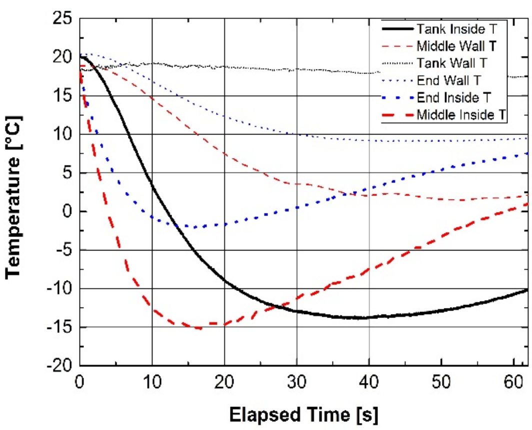


a

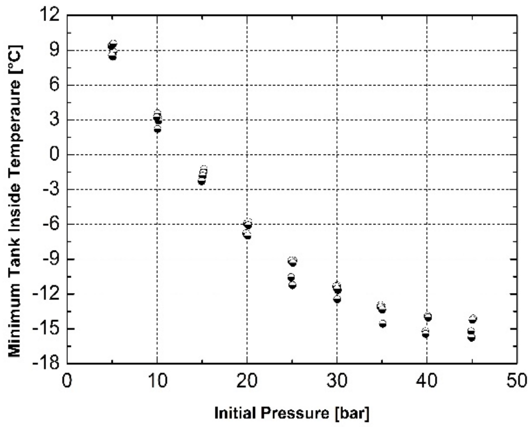


b

*Figure 3-a: Transient temperature profiles in tank, middle and end location. 40 bar depressurization. Figure 3-b: Minimum temperature inside the tank as a function of initial pressure. Depressurization from 20 °C.*

### 3.3 Pressure – temperature profile and discharge time

The local pressure – temperature profiles can be useful to assess the thermodynamic state of the $CO_2$ during the expansion and to visualize the depressurization path followed.

The expansion from 40 barg gives the pressure – temperature link represented in figure 4-a in terms of dimensionless variables. Expansion path in the tank is completely different from that at the constriction point where gradients are much more important and the dynamics faster. It should be noted that the smallest value of the temperature is not achieved at the minimum pressure but at an earlier state and, in the tank, this value arises in the final stages of the experiment. Beyond this point the gas is characterized by a heating process which is more effective at the constriction point where its rate is greater. This behaviour has been observed throughout all the trials.

Referring also to figure 3-a it is possible to see how the gaseous $CO_2$ tends to remove heat from the solid reservoir on its way to the minimum temperature. This tendency is not detectable once the thermal capacity is much greater compared to that of the gas as in the case of the tank. In fact its external wall temperature is almost constant during the trial. Therefore one may assess that in the performed trials the presence of the tank with its thermal capacity is an essential thermal driver of the expansion, affecting $CO_2$ expansion.

Trends obtained are also justified by the fact that carrying the tests the mass of the gas diminishes. In this sense the final stages are characterized by an extremely low massive gas content that is directly and rapidly heated by warmer solid walls.

Considering the ideal behavior of the gas (ensured by the compressibility factor values taken during the depressurization), it is possible to implement also a differential model consisting of an irreversible isenthalpic expansion. The basic assumption is therefore characterized by no transfer of heat and no work done with the constancy of the specific enthalpy of the substance. It is clear that both the expansion in the tank and at the constriction are far from following an isenthalpic path as indicated in figure 4-a. The latter would ideally give a progressive cooling down to a dimensionless temperature equal to 0.79 without any rise. Both the profiles are characterized by a temperature drop less pronounced also characterized by heating mechanisms already discussed. However in the dimensionless pressure range between 0.7 and 0.4 the expansion in the middle point is partly comparable with the isenthalpic path. Beyond this point it deviates significantly following the heating process. Decreasing the initial pressure, this deviation is more limited but all tests have given evidence of quite an agreement with the correspondent constant enthalpy process.

Future work will be partly focus on the implementation of a suitable model able to take into account the different contributions to the energy balance related to the profiles obtained.

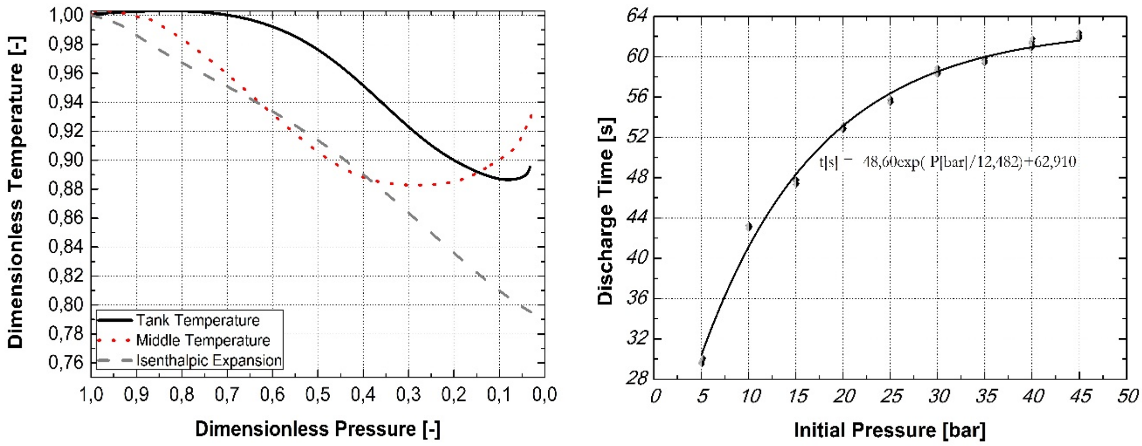


a b

*Figure 4-a: Transient pressure profiles in the tank, middle and end location. Depressurization from 40 bar. Figure 4-b: minimum temperature inside the tank as a function of the initial pressure. Depressurization from 20 °C.*

Time duration of each release has been assessed both using the DAQ internal timers as well as working on the experimental data profiles. In the latter case, the adopted criterion relies on the analysis of the pressure profiles with the starting points represented by a variation of the first derivative of the filtered profile over time.

Results obtained are collected in figure 4-b and each trial has been repeated five times under the same initial conditions.

As indicated the initial pressure plays a key role on the definition of the total discharge time here intended as the time at which the pressure inside the tank reaches the equilibrium with the outside. Figure 4-b shows clearly that an increase in the initial pressure leads to a growth in the total discharge time. Under the range investigated (5 – 45 barg at 20 °C), the increase seems to be more pronounced for the smaller initial pressure while moving to higher values tends to grow more slowly.
Data obtained can be nicely interpolated using and exponential decay shape function as plotted in figure 4-b.

## 4. Conclusions

An experimental campaign has been performed with the aim of preliminarily test an experimental apparatus to perform pressurized releases of $CO_2$. The detailed mathematical modelling of data collected is delegated to future works. Data concerning the pressure and the temperature during the depressurization have been collected in three different locations. Main conclusions are reported below.

- in the initial pressure range investigated (5 – 45 barg), depressurization profiles show a similar behaviour with main differences related to friction mechanisms. A regular depressurization profile is linked to the absence of dense – phase appearance.
- a variation in the initial CO2 pressure leads to different depressurization paths with also a direct influence on the total discharge time that is well fitted by an exponential decay shape function.
- Temperature dynamics is more complex and strictly related to both initial pressure and measurement location. Larger variations are detected at the entrance constriction point in the discharge line where therefore the expansion is supposed to be localized.
- Minimum temperature reached inside the tank shows a linear variation with the initial charging pressure up to 20 barg. But both in the tank that at the constriction point, temperature trends show a local minimum not matching the correspondence in the pressure.
- Depressurization is in fact extremely influenced by significant heat transfer mechanisms occurring with the solid stainless steel body and detected by wall thermocouples. Final expansion stages are characterized by heating processes mainly governing the phenomenon when the enthalpic contribution weakens. The main source of heat is represented by warmer solid walls and the friction flow inside the discharge line.
- The implementation of a differential irreversible isenthalpic depressurization shows significant differences from the profiles obtained except for a limited dimensionless pressure range at the constriction point.

### References

Ahmad M., Buit L., Florisson O., Hulsbosch-Dam C., Bogemann-van Osch M., Spruijt M., Davolio F., 2013a, Experimental Investigation of $CO_2$ outflow from a High-Pressure Reservoir, Energy Procedia, 37, 3005-3017.

Ahmad M., Buit L., Florisson O., Hulsbosch-Dam C., Bogemann-van Osch M., Spruijt M., Davolio F., 2013b, Study of the thermohydraulics of CO2 discharge from a high pressure reservoir, Int. J. of Greenhouse Gas Control, 19, 63-73.

Martynov S., Brown S., Mahgerefteh H., Sundara V., 2013, Modelling choked flow for $CO_2$ from the dense phase to below the triple point, Int. J. of Greenhouse Gas Control, 19, 552-558.

Mocellin P., Vianello C., Maschio G., 2015, Carbon Capture and Storage Hazard Investigation: Numerical Analysis of Hazards related to Dry Ice Bank Sublimation following Accidental Carbon Dioxide Releases, Chemical Engineering Transactions, 43.

Vianello C., Macchietto S., Maschio G., 2012, Conceptual Model for $CO_2$ release and risk assessment: a review, Chemical Engineering Transactions, 26, 573-578, DOI: 10.3303/CET1226096.